OPTICAL AND DIELECTRIC PROPERTIES OF ZnO NEMATIC LIQUID CRYSTALS PREPARED BY THE CHEMICAL PRECIPITATION METHOD**

K. V. S. N. Raju [1], Sk. S. Begum [2], B. T. P. Madhav [3], M. C. Rao [4*]

[1] Department of Physics, Koneru Lakshmaiah Educational Foundation, Vaddeswaram, India
[2] Department of Physics, NRI Institute of Technology, Pothavarappadu, India
[3] Antennas and Liquid Crystals Research Center, Department of ECE,
Koneru Lakshmaiah Education Foundation, Vaddeswaram, India
[4] Department of Physics, Andhra Loyola College, Vijayawada, India;
e-mail: raomc72@gmail.com

Mesogenic 4-pentyl-4'-cyanobiphenyl (5CB) is a commonly used dielectric material for display devices and liquid crystal biosensors. A small concentration of ZnO nanoparticles was dispersed in 5CB nematic liquid crystals by the chemical precipitation method. The phase changes, phase retardation, and transition temperature of the prepared samples were studied by polarizing optical microscopy (POM) and differential scanning calorimetry analysis. The dielectric properties were measured by dielectric spectroscopy, which was performed within the frequency range from 1 Hz to 10 MHz. A novel phase was identified and confirmed by the dielectric parameters in dispersed ZnO 5CB (N5CB). Specifically, the temperature dependence of relaxation times was estimated for both the samples, which strengthen the POM studies and the influence of nanoparticles on the lattice arrangement. The temperature dependence and the dispersion effect of ZnO nanoparticles on the dielectric constant and dielectric losses were also studied. The sensitivity of mesogenic phases to external forces was confirmed through the present work. From all these results, it has been concluded that N5CB finds potential application in the preparation of fast switching devices.

Keywords: *liquid crystals, ZnO nanoparticles, polarizing optical microscopy, dielectric permittivity, dielectric constant, relaxation time.*

ОПТИЧЕСКИЕ И ДИЭЛЕКТРИЧЕСКИЕ СВОЙСТВА НЕМАТИЧЕСКИХ ЖИДКИХ КРИСТАЛЛОВ ZnO, ПОЛУЧЕННЫХ МЕТОДОМ ХИМИЧЕСКОГО ОСАЖДЕНИЯ

K. V. S. N. Raju [1], Sk. S. Begum [2], B. T. P. Madhav [3], M. C. Rao [4*]

УДК 543.42;620.3

[1] Отделение физики Образовательного фонда Конеру Лакшмайя, Ваддесварам, Индия
[2] Технологический институт NRI, Потхавараппаду, Индия
[3] Исследовательский центр антенн и жидких кристаллов
Образовательного фонда Конеру Лакшмайи, Ваддесварам, Индия
[4] Колледж Андхра Лойола, Виджаявада, Индия; e-mail: raomc72@gmail.com

(Поступила 12 июля 2021)

В нематические жидкие кристаллы 4-пентил-4'-цианобифенила (5CB) методом химического осаждения диспергированы наночастицы ZnO небольшой концентрации. Фазовые превращения, фазовое замедление и температура перехода образцов исследованы методами поляризационной оптической микроскопии и дифференциальной сканирующей калориметрии. Диэлектрические свойства определены методом диэлектрической спектроскопии в диапазоне частот 1 Гц–10 МГц. Новая фаза идентифицирована и подтверждена диэлектрическими параметрами в диспергированном ZnO 5CB (N5CB). Оценены температурная зависимость времени релаксации для образцов и влияние наноча-

**Full text is published in JAS V. 89, No. 3 (http://springer.com/journal/10812) and in electronic version of ZhPS V. 89, No. 3 (http://www.elibrary.ru/title_about.asp?id=7318; sales@elibrary.ru).

стиц на расположение решетки. Исследованы температурная зависимость и влияние дисперсии наночастиц ZnO на диэлектрическую проницаемость и диэлектрические потери. Установлена чувствительность мезогенных фаз к внешним воздействиям. Сделан вывод о перспективах применения N5CB при изготовлении быстродействующих коммутационных устройств.

Ключевые слова: *жидкий кристалл, наночастица ZnO, поляризационная оптическая микроскопия, диэлектрическая проницаемость, диэлектрическая постоянная, время релаксации.*

Introduction. In the current world, highly effective energy storage devices have attracted much attention [1–7]. The technology of energy storage includes fuel cells, Li-ion batteries, molten salt, flywheel, pumped hydro-storage, super capacitor, etc. All these devices require varieties of materials to store the energy in various forms. Our previous studies revealed that liquid crystals are one of the materials suitable for energy storage [8, 9]. To check the compatibility of the material for energy storage, a knowledge of dielectric parameters is required. Mesogenic 4-pentyl-4′-cyanobiphenyl (5CB) is the commonly used dielectric material for display devices and liquid crystal biosensors. It exists in the nematic phase at room temperature and is liquefied at 35°C. Nematogen is the common name for nematic liquid crystalline materials. Changing properties of 5CB in the presence of foreign elements, even at low concentrations, attract the interest of researchers. Biomolecules and nanoparticles play a major role in achieving and enhancing the desired properties for the application of 5CB. Analyzing the novel behavior of doped mesogens requires various techniques, including dielectric studies.

Semiconducting nanoparticles such as ZnO nanoparticles in liquid crystal (LC) mixtures have been employed as dopants in condensed optical materials intended for novel optoelectronic devices. It is well known that dielectric studies of LC materials possess a valuable source of information on their molecular arrangement and intermolecular interactions, in both mesomorphic and isotropic phases. So, most of the researchers in this field investigate the dielectric properties of LC materials, both experimentally and theoretically [10, 11]. The analysis of dielectric data certainly informs the researcher about the application of the LC material in the presence of the electric field, which is vital for storage devices, light modulators, and display devices. ZnO nanoparticles have different device applications such as light detectors, LEDs, photo sensors, solar cells, etc. [12]. By adding ZnO nanoparticles to liquid crystals, their textures, temperature, phase transition and electro-optical parameters will be modified. The variation of transition temperatures, novel phase, and predominant change in the dielectric properties helped us to state that ZnO nanoparticles have a significant effect on the physical properties of pure 5CB. A lower relaxation time of samples means that it quickly responds to the external field and gives stabilization at a fast rate. This in turn leads to a low consumption of power. The addition of metal oxide nanoparticles to nematic mesogens has improved the alignment properties of LC systems [13].

The present work reports dielectric parameters (dielectric permittivity (ε′), dielectric loss (ε″), and relaxation time (τ)) as well as transition temperatures through these studies for pure 5CB and dispersed ZnO 5CB (N5CB). The studies reveal advantages of N5CB over pure 5CB in the field of engineering in specific storage devices. Moreover, we use polarizing optical microscopy (POM) and phase retardation obtained from image analysis using MATLAB. It should be noted that we focus on analyzing the thermal, optical, and dielectric properties using the chemical precipitation method in mesogenic systems by the dispersion of ZnO nanoparticles. The experimental outcomes are analyzed in detail.

Experimental. *Materials.* The nematic liquid crystal materials used in the present investigation are 5CB and the dispersed nanomaterial is ZnO. The phase transitions of these materials are mentioned below.

$$\text{5CB Crystal} \xleftrightarrow{25^\circ\text{C}} \text{N} \xleftrightarrow{38^\circ\text{C}} \text{I}$$

$$\text{N5CB Crystal} \xleftrightarrow{25^\circ\text{C}} \text{Smectic C*} \xleftrightarrow{175^\circ\text{C}} \text{N} \xleftrightarrow{350^\circ\text{C}} \text{I}$$

The 5CB (99% purity) was received from Merck (Singapore). Micro glass slides were obtained from Fisher Scientific (USA). ZnO nanoparticles were prepared from zinc nitride [$Zn(NO_3)_2 \cdot 6H_2O$] and NaOH (Merck). These chemicals were dissolved in distilled water to form 100 mL of alkaline zinc solution [Zn^{2+} = 0.5M, OH = 1.0 M] [9]. The ITO-coated glass cell designed by INSTEC Company was used to place the sample under study. The dimension of the cell used was 5mm×5mm×5μm. The thickness of the sample was 5 μm (cell gap).

Preparation of the samples. Pure 5CB was commercially bought and used. ZnO nanoparticles of 35 nm in size were prepared in our laboratory through the chemical precipitation method, which was explained in

our previous publications [8, 9]. These nanoparticles were dispersed in the host 5CB lattice in the liquid phase at a 1 wt.% ratio. Then the mixture consisting of 5CB dispersed with ZnO nanoparticles was placed on the stirrer at 40°C for 1 h to obtain uniform distribution of nanoparticles in the 5CB lattice. The final mixture was named N5CB. One speck of this N5CB was placed on a previously rubbed micro glass slide and then sealed by carefully placing a glass sticker to obtain uniform alignment of the sample. Then the sample-filled glass slide was placed in a hot stage connected to a dimmer stat, to vary the temperature [9]. The sample was taken over a normal glass slide for the POM study. Before placing the sample on a glass slide, it was rubbed in one direction to avoid more irregularities in the orientation of the sample. The uniform alignment of the sample leads to the maximum optical polarization of the input light. Initially, the polarizers of the POM were in a crossed position, and no light was observed by the author. But when the uniformly aligned sample was placed between these two polarizers, then, because of the anisotropic nature of the sample the input light was polarized to another angle as per the orientation of the molecules of the sample, thus leading to observation of the surface orientation of the molecules. This is nothing but the texture of the sample. Also, the size of the nanoparticles used here was fixed at 35 nm. The concentration of doping used in this work was in the order of 1 wt.%. The sample of liquid crystal (5CB) taken weighed 1 g, and the ZnO nanoparticles taken weighed 0.001 mg.

Methodology. A Meopta polarizing optical microscope was used to observe the textures and phase transitions of the samples. The phase changes were captured using a Nikon camera of 64 Mp attached to the microscope. The image analysis technique was employed to these textures to obtain the phase retardation using MATLAB software. Dielectric measurements were made for these samples through Newton's 4th Ltd., LCR meter (Model PSM1700) within the frequency range 1 Hz–10 MHz. This LCR meter is a computer controlled device and gives the values of capacitance, resistance, and inductance for the given inputs of voltage and frequency. The procedure of taking dielectric data from the above-mentioned inductance, capacitance, resistance (LCR) meter was repeated at different temperatures of the sample, which is kept on a computer-controlled INSTEC hot plate. The measurements in the cell with homeotropic alignment gave us the value of ε', parallel to the director of the LC. The temperature stability within the measurement was better than ±0.1°C. At frequencies less than 10 Hz absorption due to the ionic conductivity of the LC can be observed. It should be noted that ZnO nanoparticles do not absorb the electric field in the observed frequency range, their absorption bands lie at $f > 10$ MHz. Therefore, data at $f > 10$ MHz are omitted [14–20].

The retardation in the liquid crystal phase of the sample is obtained using phase retardation (δ). The equation for phase retardation is:

$$\delta = \frac{2\pi dn}{\lambda}. \tag{1}$$

The dielectric constant is defined as the ratio of capacitance with the dielectric material to the capacitance in a vacuum. Practically, the dielectric constant (ε') is obtained using the following equation (2):

$$\varepsilon' = \frac{(c_p - c_0)d}{\varepsilon_0 A} + 1, \tag{2}$$

where A is the area of the capacitor cell, d is the thickness of the cell, ε_0 is the permittivity of free space = $= 8.85\times10^{-12}$ F/m, c_p is the capacitance with the dielectric material, and c_0 is the capacitance without the material.

For an electric field, the molecules of the LC sample experience the loss of absorbed energy owing to orientation polarization. These energetic losses are called dielectric losses. They can be obtained directly from tan δ values collected from the LCR meter using the equation:

$$\varepsilon'' = \varepsilon' \tan\delta. \tag{3}$$

The relaxation time (τ) is calculated using Slater's perturbation:

$$\tau = \tan\delta/\omega, \tag{4}$$

where $\omega = 2\pi f_0$ and f_0 is the resonance frequency.

With the help of above equations, the relaxation times are calculated for the selected samples (5CB and N5CB) at different temperatures starting with the liquid crystal phase and ending with the liquid phase.

Results and discussion. *POM studies.* Transition temperatures of 5CB and N5CB were observed through polarizing optical microscopy and confirmed through the present dielectric studies. The same are mentioned in Table 1. A novel texture of Smectic C* was observed in N5CB in the temperature range 30–175°C. These static values of the 5CB compound are in good agreement with several previously reported

values in the literature [21, 22]. The texture of N5CB observed through a normalized polarizing optical microscope within the temperature range 30–175°C was shown in Figs. 1a and b. The plate number 162 matches the maximum extent of the image observed for the sample N5CB. Of course, its Smectic C twisted phase is represented with SmC*. The achiral 5CB was influenced by the ZnO nanoparticles near their lattice positions and hence metallomesogens [23] resulted in obtaining the chirality in the molecular positions of the 5CB. The images obtained from POM were included here. Fig. 1a represents the Smectic phase of the N5CB, which gives the surface orientation of molecules and not the aggregation of the ZnO nanoparticles. The composite formed because of the dispersion of ZnO nanoparticles and 5CB tends to align in the twisted layered structure as SmC*. The dots over the slippery-like structure represent the claimed phase of the N5CB. Also, in Fig. 1b, it is very clear that nematic droplets are observed owing to the thermal energy change and transition phase. The results of the transition temperatures of N5CB indicate that the dispersed ZnO nanoparticles have extremely reoriented the host and extend the LC phase up to a high thermal range. This extraordinary behavior can be explained based on the continuum theory that supports the interactions of nanoparticles with the nematic LC and was beautifully explained in the literature [24].

TABLE 1. Transition Temperatures of 5CB and N5CB

Sample	Study	T_{CN}, °C	T_{NI}, °C
5CB	POM	25	38
	DSC	25	36
	Dielectric study	26	38
N5CB	POM	30 (T_{CSmC*}) 175 (T_{SmC*N})	290
	DSC	31 (T_{CSmC*}) 173 ($T_{SmC*N)}$	296
	Dielectric study	32 (T_{CSmC*}) 170 (T_{SmC*N})	308

N o t e. POM polarizing optical microscopy, DSC differential scanning calorimetry.

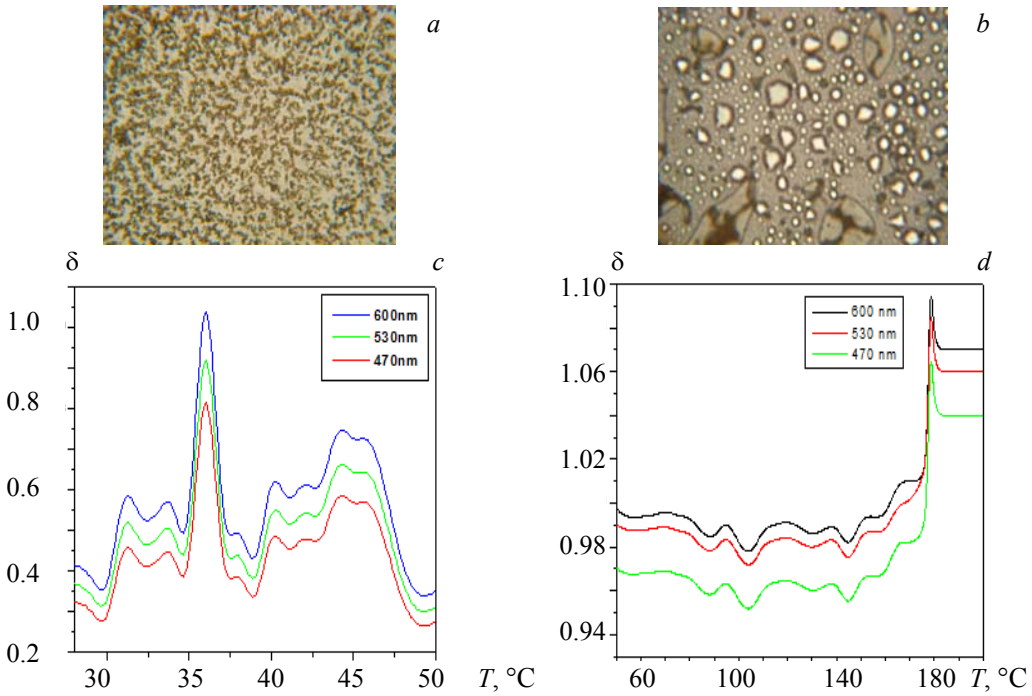

Fig. 1. (a) SmC* phase of N5CB at 100°C, (b) nematic phase of N5CB at 270°C, and the temperature dependence of phase retardation (δ) for (c) 5CB, (d) N5CB.

The snapshots of 5CB and N5CB taken at various temperatures of the LC phase are analyzed using MATLAB software to study phase retardation [9]. The plots of phase retardation (δ) vs temperature in the LC phase of the samples 5CB and N5CB are shown in Figs. 1c and d. The values of δ are calculated for three different wavelengths (470, 530, and 600 nm) in the optical region for both the samples. From the phase retardation of the samples, it is observed that the behavior of phase retardation is changed; namely, it increases with temperature up to the phase of the LC and then decreases when there is a phase transition. In Fig. 1c, two significant peaks are visible within a short span of temperature. This shows the most unstable nature of the 5CB LC to external thermal energy. However, the strong phase retardation is observed in N5CB up to a large temperature range. This is an interesting point and is shown in Fig. 1d. The birefringence is not equal to zero for LC [25]. The refractive index of the sample in the isotropic phase is between the values of the refractive indices of ordinary and extraordinary rays. In this paper, the birefringence is calculated using the image analysis method through MATLAB. The phase retardation is calculated using Eq. (1). The LC phase of N5CB is for a long duration of temperature, and the most stable compound is obtained through this method of chemical precipitation. This also confirms the POM and other studies of this communication.

DSC analysis. Differential scanning calorimetry (DSC) was performed on the studied samples, 5CB and N5CB (with 1 wt.% of ZnO), to analyze the change in phase transition temperatures. The heating scan of the DSC for all the samples is shown in Fig. 2. From the DSC, the thermograms represent the heat flow transition and the predominant peaks were identified as phase transitions of the sample. The appearance of very small peaks in the DSC thermograms is assigned to noise of the instrumentation. Here, a single peak observed in 5CB corresponds to the transition of the nematic phase to the isotropic phase. For a lower concentration of the ZnO mixture (1 wt.%) two distinct peaks were observed at 171.3 and 296.79°C. The first peak reports the transition of the ordered Smectic C* to the disordered nematic phase. The second peak is due to the existence of localized semi-nematic domains where the mixture possesses the orderly alignment stipulated by ZnO nanoparticles. The rise in $T_{\text{Iso-N}}$ and the occurrence of a second peak in the DSC thermogram of N5CB (Fig. 2b) is due to the blending of the ZnO and 5CB molecules. Therefore, the effect of ZnO nanoparticles on the liquid–nematic transition temperature ($T_{\text{Iso-N}}$) depends on the selection of the host and the concentration of ZnO nanoparticles. This study helped us to support the local short-range orientation of N5CB molecules around the ZnO nanoparticles because of its anchoring energy. This novel state is also called the paranematic state.

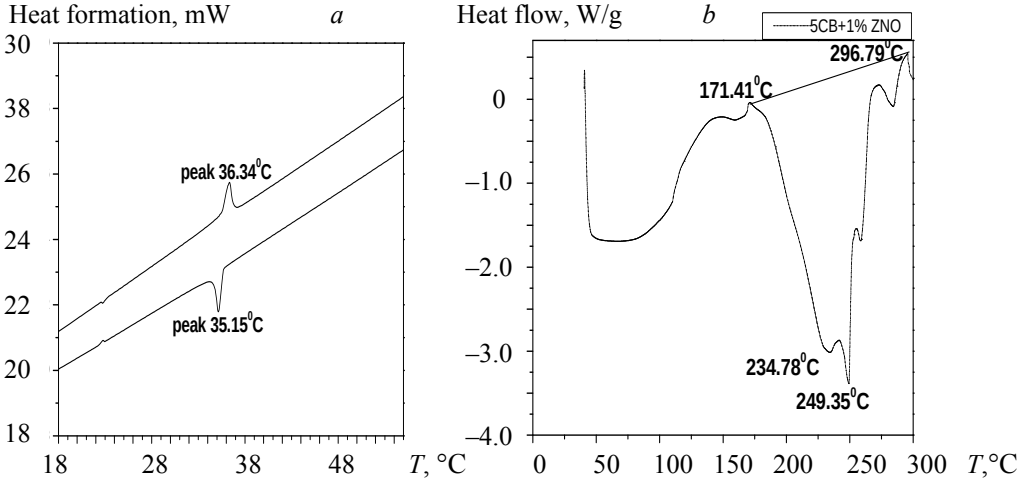

Fig. 2. Differential scanning calorimetry thermograms of (a) 5CB, (b) N5CB.

Dielectric studies. The studies involve the measurement of dielectric permittivity, dielectric loss, and the temperature coefficient of the dielectric constant within the frequency range 1 Hz–10 MHz for 5CB and N5CB samples (Figs. 3–5). The dispersion of ZnO nanoparticles with nematic LC caused appreciable changes in the spectra. Figure 3a shows the plots of dielectric permittivity vs frequency at different temperatures of the samples. Figure 3b shows the plots of dielectric loss vs frequency at different temperatures of the samples. The pure 5CB and its nano-nematic composite system of the dielectric constant at different temperatures are depicted in Figs. 3a,b, respectively. It is interesting to note that the maximum value of the dielectric

constant is 53.69 at a low frequency and decreases gradually with increasing frequency, but we see a slight increase in its numerical value with increasing temperature. The large values of the dielectric constant at low frequencies are due to orientational polarization. This variation of the dielectric permittivity as a function of frequency can be explained by Koop's theory, in which dielectric materials are treated as a two-layer structure of the Maxwell–Wagner type. In this model, one layer is a conducting layer that is attributed to the grains, and the second layer is a weak conducting layer assigned to the grain boundaries of the material. The grains play a significant role at high frequencies owing to their small dielectric constant values. However, the observed dielectric properties are mainly due to the high values of the dielectric constant for grain boundaries. This behavior is almost the same as that reported by other studies.

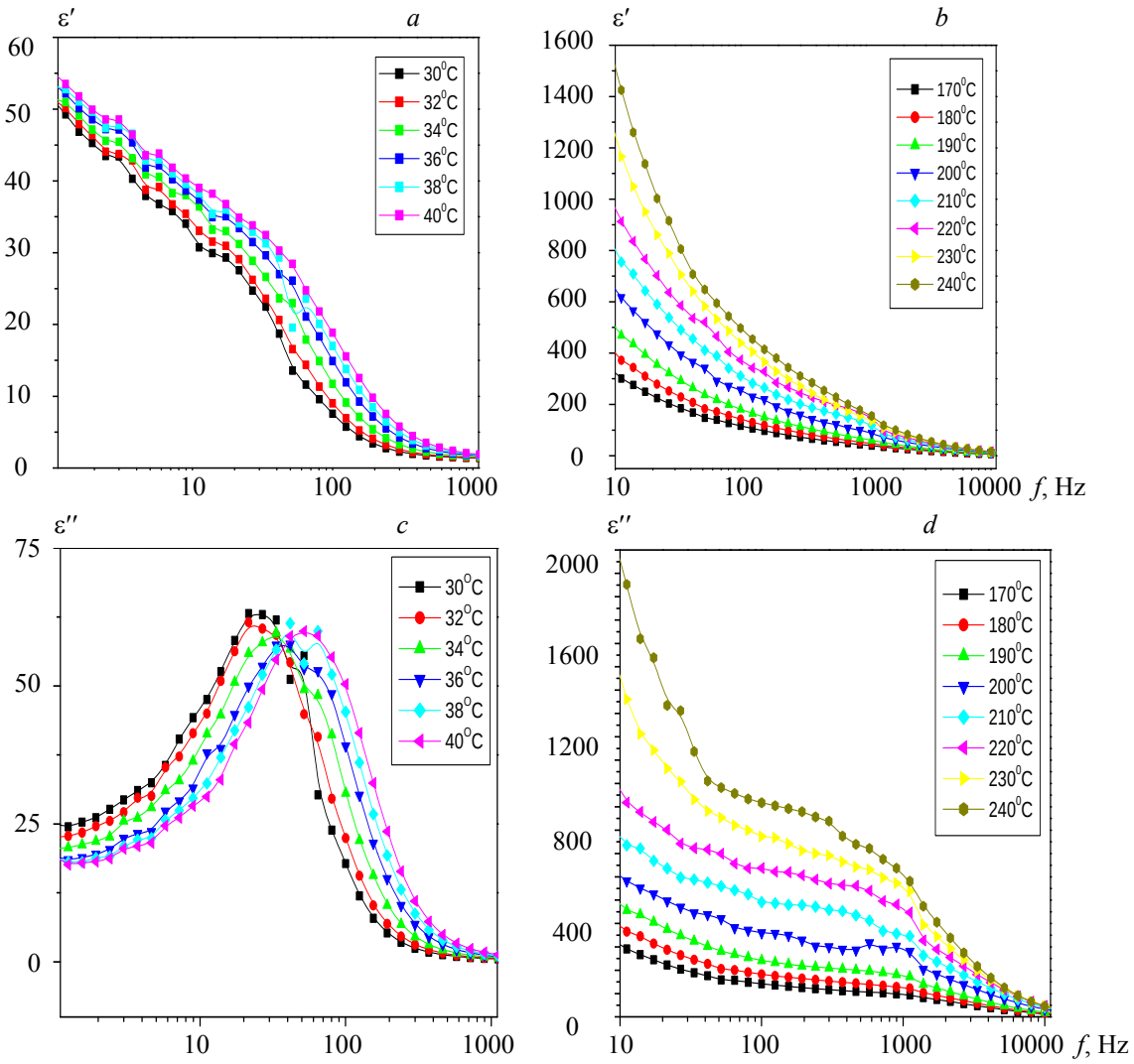

Fig. 3. Frequency dependence of dielectric constant ε′ for (a) 5CB, (b) N5CB, and dielectric loss ε″ for (c) 5CB, (d) N5CB.

The dielectric analysis of the studied samples was carried out within the frequency range 1 Hz–10 kHz with varying temperature. An LCR meter was operated for data collection for every 2°C temperature of the sample (both for 5CB and for N5CB). The data obtained from this LCR meter were in terms of capacitance and tan δ, which afterward were used to calculate the dielectric constant (ε′), dielectric loss (ε″), and relaxation time (τ) using Eq. (2)–(4), respectively. The obtained data are visualized in the form of plots, as in Figs. 3–5. The temperature variation of dielectric parameters helped to confirm the transition temperatures of the studied samples. The sudden change in the behavior of the dielectric parameter revealed the transition of the phase of the sample at that particular temperature. The dielectric constant of ZnO nanoparticle 5CB sys-

tems increased compared with pure 5CB. It is because the dipole moment of the ZnO nanoparticle is higher than for the nematic liquid crystal molecule system [26]. Figures 3c and d clearly indicate that the dispersion of ZnO nanoparticles is dependent on the dielectric constant and the dielectric loss of the host system. Moreover, we obtained that the dispersion of ZnO nanoparticles influences the rotation of LC molecules around their short axes and shifts the absorption bands to lower frequencies; meanwhile, the amplitude and width of the absorption bands increase. This result confirms that dispersed nanoparticles strongly interact with the LC molecules owing to their large dipole moment and high polarizability. The nanoparticles affect both dielectric constant and dielectric loss of the system. The rise in the dielectric constant for N5CB can be understood as the matching of dipole moments of ZnO nanoparticles and 5CB resulting in uniform orientation. In the presence of the low-frequency electric field, the ionic polarization persists in N5CB and results in the enhancement of dipole moments.

In Figures 3c and d the dielectric constants and dielectric losses of the samples 5CB and N5CB are shown as a function of frequency (over the log scale) ranging from 1 Hz to 1 MHz. The data plotted in these figures is against different temperatures of the samples in their nematic phase only. Of course, the temperatures of 5CB and N5CB used to plot the Figs. 3c,d are not within the same range; however, they are considered to observe the behavior of the samples in their nematic state. Also, from these plots, the salient observations made, namely, the dielectric constant and dielectric loss of N5CB always have high values compared with 5CB at all temperatures for any particular frequency of the input signal. That indicates that the dielectric nature of N5CB is stronger than that of 5CB. This is attributed to the inclusion of ZnO nanoparticles in the lattice of 5CB. It should be noted here that the metallic nature of ZnO (conductor) is modified for nano sizes, which helps to enhance the insulating behavior of the host lattice. Moreover, the temperature ranges of the LC state are different for 5CB and N5CB.

The temperature dependence of the dielectric constant at different frequencies for the pure 5CB and dispersed ZnO material (N5CB) is shown in Figs. 4a and b. From Fig. 4a, we see that the variation of the dielectric constant is linear at low frequencies (up to 100 Hz) with increasing temperature, whereas for N5CB, the same dependence is nonlinear (up to 1 kHz). This change is due to the presence of nanoparticles. The transition temperatures ($T_{N\text{-}I}$) of 5CB obtained from the dielectric studies (5CB 38°C) is slightly different from the DSC studies (5CB 36°C) and the POM studies (5CB 40°C). At lower frequencies there is a sharp increase when the transition from solid to smectic C* for dispersed ZnO materials takes place. The transition temperatures are confirmed significantly through dielectric constant curves. However, all these changes are seen at lower applied frequencies up to 100 Hz. There are four types of dielectric polarization, viz., electronic polarization, ionic polarization, dipolar or orientational polarization, and space-charge polarization. Among these, the first three types of polarization can be exhibited by the sample under study to give different applications. The applied AC electric field with varying frequency is maintained in such a way that the samples will not suffer by space-charge polarization as it leads to damage (it will be observed only when the sample is under high voltages). Hence, generally, electronic, ionic, and dipolar polarizations of the sample are considered. For some important cases, the behavior of the samples at different frequencies can be explained within the theory of dipolar polarization [27]. Polarization of dipoles in the region of 1 kHz frequency is dipolar polarization, which is also named orientational polarization. For the frequency range studied in this paper, the molecular structure of 5CB can be described as a dipole structure. Thus, the studied samples exhibit orientation polarization rather than ionic and electronic polarizations [28–30]. Figure 4 shows a graph of dielectric loss as a function of temperature at selected frequencies. At lower frequencies, the dielectric loss increases with the temperature and reaches a peak value, and then the losses decrease with a further increase in temperature for both the samples. At higher frequencies with an increase in temperature the peak decreases and becomes almost constant for both samples. There is a sharp increase in the dielectric loss when the transition from solid to smectic C* takes place.

The dielectric constant depends on the dielectric polarization of the sample, which in turn depends on the frequency of the input signal. As the samples studied in the present manuscript have a long molecular structure with covalent bonds between the organic atoms, the response of these molecules to the external electrical field depends on the frequency of the signal. At lower frequencies of the input signal, the molecular structure of 5CB and N5CB respond through orientation and give dipolar polarization, thus giving a high dielectric constant. At a high frequency of the input signal, the variation of the electric field vector changes rapidly, which the molecular structure of the samples cannot support to give stable polarization, and hence the polarization decreases, which leads to a low dielectric constant of 5CB at a high frequency (>1 kHz). Also, the dielectric polarization of the sample depends on its phase. Here, in the nematic phase the order of the

molecules are moderate, giving some dielectric polarization, and at a temperature near T_{NI} (isotropic phase) the molecules are completely disordered, giving a stable dielectric constant. Hence, at high temperatures, the samples exhibit a low dielectric constant. In Figure 4b, the dielectric constant is very small but not less than 1 as the graph is in a higher order and cannot be visualized when compared to low frequency. The transition temperatures are confirmed significantly through dielectric loss curves.

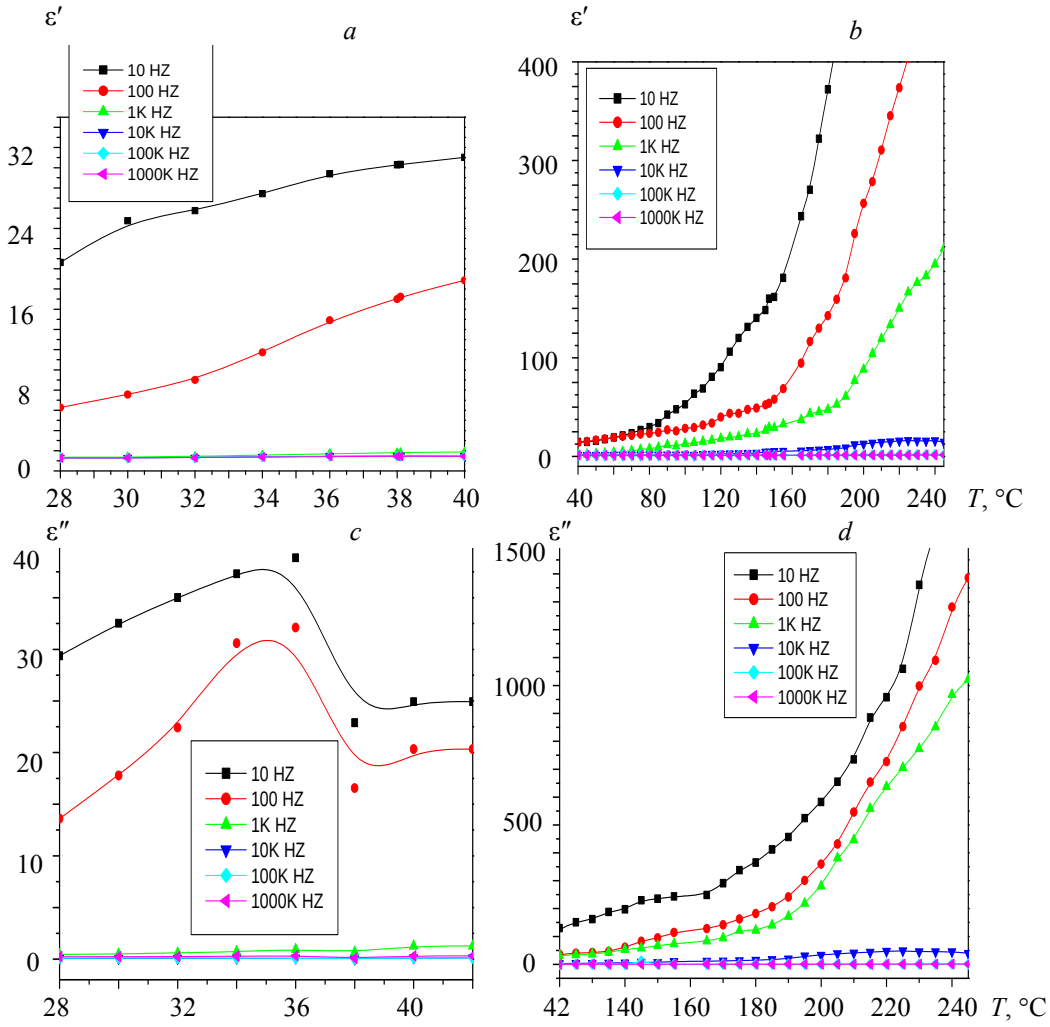

Fig. 4. Temperature dependence of dielectric constant ε′ for (a) 5CB, (b) N5CB, and dielectric loss ε″ for (c) 5CB, (d) N5CB.

Figures 5a and b show the variation between the dielectric constant and the dielectric loss plotted at different temperatures for pure and dispersed ZnO 5CB. The values of ε′ and ε″, corresponding to the peak of the plot, are identified and related to the frequency, which is used to determine the relaxation time (Table 2). Table 3 specifically represents their relaxation frequencies (f_0) and relaxation times (τ) in the nematic phase of the samples. These Cole–Cole plots show Debye relaxation. The calculated relaxation times are in good agreement with that obtained from these plots. The Debye theory of dielectric relaxation is applicable to liquids. Martin et al. [31] have extended the Debye theory of dielectric relaxation in liquid to the nematic and have shown that the relaxation time in LCs is larger than the ordinary Debye relaxation time T_D by a factor $g = \frac{-kt}{4}\exp\left(\frac{L}{kT}\right)$ [32, 33]. This procedure is repeated for all temperatures of the samples in their liquid crystalline planes. Similarly, the temperature influence was also observed on the samples in terms of the relaxation time. For both the studied samples, the relaxation time decreased with the temperature. The basic lattices of the samples are almost the same, but varied with the presence of nanoparticles. The authors compared the samples in their respective mesogenic (liquid crystalline state) phase. The 5CB sample exists in the

mesogenic phase at low temperatures only (<40°C). Hence, the comparison cannot be drawn by merely taking high temperatures, but by taking the same state of matter. The calculated relaxation times (τ) for 5CB and N5CB are again plotted with the temperature, as shown in Figs. 5c and d. Figure 5c shows the decrease in the relaxation time with increasing temperature owing to the thermal vibrations in the pure mesogens. This leads to weak intermolecular forces and thus a lower relaxation time through low cohesive energy and internal pressure. However, Fig. 5d shows a significant relaxation time at a temperature around 175°C. This is assigned to the change in the molecular alignment of N5CB, which is also reflected in the POM studies as the transition from Smectic C* to the nematic phase. Thus, dielectric studies correlate with the POM studies and help to strengthen the phase transition temperatures of the prepared sample.

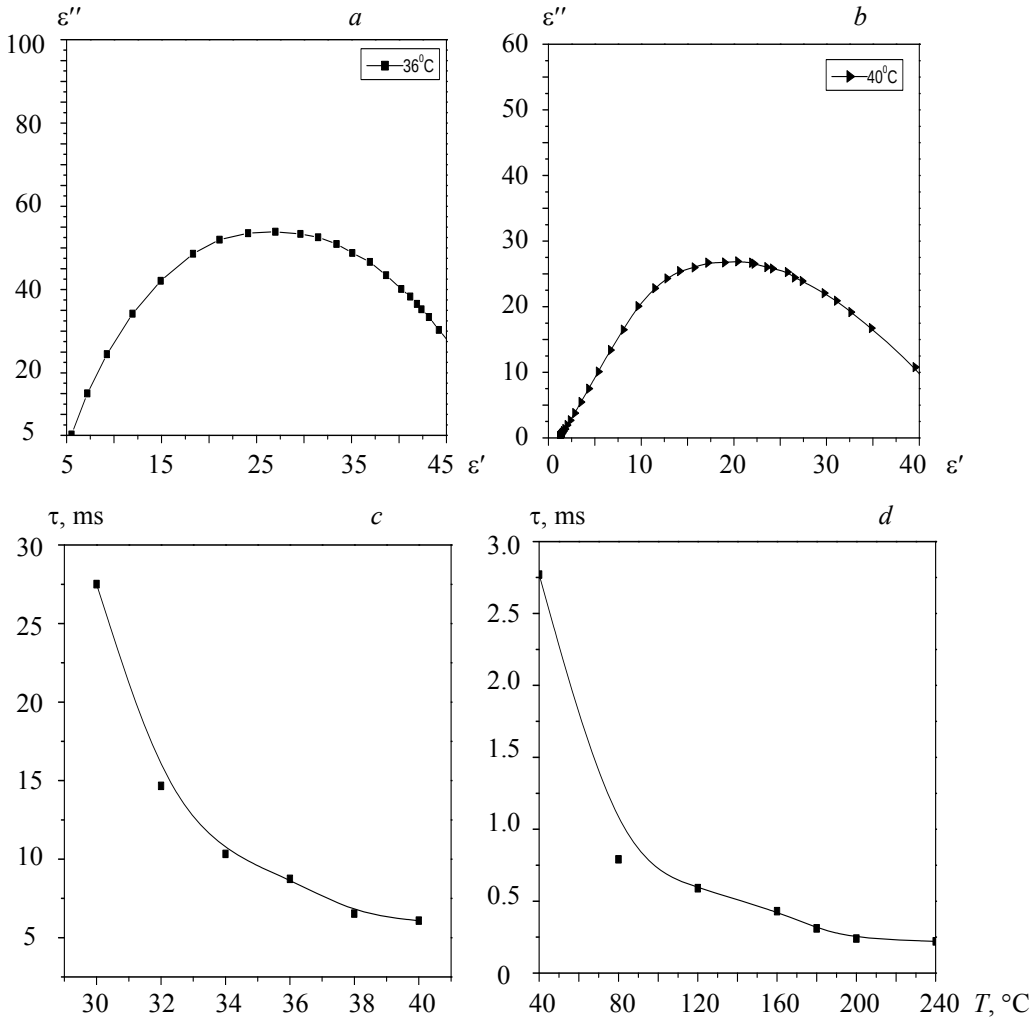

Fig. 5. Variation between dielectric constant ε′ and dielectric loss ε″ of (a) 5CB, (b) N5CB, and temperature dependence of τ for (c) 5CB, (d) N5CB.

TABLE 2. Relaxation Times of 5CB and N5CB in the Nematic Phase

5CB		N5CB	
T_{NI}, °C	τ, ms	T_{NI}, °C	τ, ms
30	27.51	40	2.77
32	14.66	80	0.79
34	11.31	120	0.59
36	8.74	160	0.43
38	6.53	180	0.31
40	6.07	200	0.24

TABLE 3. Relaxation Frequency and Relaxation Time of 5CB and N5CB

Sample	T, °C	f_0, Hz	τ, ms
5CB	32	51	14.66
N5CB	175	700	0.52

Conclusions. ZnO nanoparticles are dispersed in 5CB nematic LCs using the chemical precipitation method. All the results are analyzed systematically by the comparative study of 5CB and its nano-dispersed counterpart. The studied samples show significant features in terms of textures, phase retardation, the dielectric constant, relaxation time, and temperature coefficient of the dielectric constant. Pure 5CB exists only in the nematic phase; however, ZnO nanoparticles have influenced the lattice of 5CB and made it exhibit the texture of Smectic C*. This feature guides us to conclude that the dispersed nanoparticles have not only changed the direction of molecular orientation but also made it rotate layer by layer. Further, the dielectric parameters of N5CB are found to be high, indicating more dielectric strength of the material. The most interesting findings of the present work are the significant decrease in the relaxation time of 5CB owing to the presence of ZnO nanoparticles. This is attributed to the high activity of nano-sized ZnO. A gradual decrease in the relaxation time in 5CB and a significant peak in N5CB temperature are also inferred in the new phase. The sensitivity of mesogenic phases to external forces is confirmed through the present work. The variation of transition temperatures, novel phase, and predominant change in the dielectric properties helped to state that ZnO nanoparticles have a significant effect on the physical properties of pure 5CB. Based on this, it is concluded that the studied samples have an important part to play in the preparation of fast switching devices.

REFERENCES

1. A. Achour, R. L. Porto, M. Akram Soussou, M. Islam, M. Boujtita, K. Ait, A. Djouadi, T. Brousse, *J. Power Sour.*, **300**, 525–532 (2015).
2. X. Wang, P. See Lee, *J. Mater. Chem. A*, **3**, 21706–21712 (2015).
3. Q. Ke, J. Wang, *J. Materiomics*, **2**, 37–54 (2016).
4. S. Sampath, D. D. Sarma, A. K. Shukla, *ACS Energy Lett.*, **1**, 1162–1164 (2016).
5. O. Muntesharia, J. Lauc, A. Krishnana, B. Dunnc, L. Pilon, *J. Power Sour.*, **374**, 257–268 (2018).
6. A. Armutlulu, L. A. Bottomley, S. A. Bidstrup Allen, M. G. Allen, *Chem. Electrochem.*, **2**, 236–245 (2014).
7. L. N. Jin, F. Shao, C. Jin, J. N. Zhang, P. Liu, M. X. Guo, S. W. Bian, *Electrochim. Acta*, **249**, 387–394 (2017).
8. S. Sreehari Sastry, S. Salma Begum, T. Vindhya Kumari, V. R. K. Murthy, S. T. Ha, *Asian J. Chem.*, **9**, 2462–2471 (2012).
9. K. V. Surya Narayana Raju, S. Salma Begum, B. Dharma Sagar, S. Babu, *Rasayan J. Chem.*, **10**, 37–45 (2017).
10. A. K. Srivastava, A. K. Misra, P. B. Chand, R. Manohar, J. P. Shukla, *Phys. Lett. A*, **37**, 490–498 (2007).
11. R. Manohar, S. P. Yadav, A. K. Srivastava, A. K. Misra, K. K. Pandey, P. K. Sharma, A. C. Pandey, *Jpn. J. Appl. Phys.*, **48**, 101501–101506 (2009).
12. J. L. Gomez, O. Tigli, *J. Mater. Sci.*, **48**, No. 2, 612–624 (2013).
13. M. Chaari, A. Matoussi, *Phys. B Condens. Mater.*, **407**, 3441–3447 (2012).
14. P. G. Cummins, D. A. Dunmur, D. A. Laidler, *J. Mol. Cryst. Liq. Cryst.*, **30**, 109–123 (1975).
15. A. Bogi, S. Faetti, *J. Liq. Cryst.*, **28**, 729–739 (2001).
16. V. A. Greanya, A. P. Malanoski, B. T. Weslowski, M. S. Spector, *Liq. Cryst.*, **32**, 933–941 (2007).
17. S. I. Zhou, K. Neupane, Y. A. Nastishin, A. R. Baldwin, S. V. Shiyanovskii, O. D. Lavrentovich, S. Sprunt, *Liq. Cryst.*, **10**, 6571–6581 (2017).
18. S. Mohyeddine, M. B. Pandey, D. Revannasiddaiah, *Phase Trans.*, **82**, 11–18 (2009).
19. M. A. Bates, G. R. Luckhurst, *Mol. Phys.*, **99**, 1365–1371 (2001).
20. C. Wakai, A. Oleinikova, M. Ott, H. Weingärtner, *J. Phys. Chem. B*, **109**, 17028–17030 (2005).
21. A. Hourri, T. K. Bose, J. Thoen, *Phys. Rev. E*, **63**, 051702 (2001).
22. B. J. Thoen, T. K. Bose, *Handbook of Low and High Dielectric Materials and their Applications*, H. S. Nalwa Academic Press, San Diego, **1**, 501–561 (1999).
23. K. Rajendiran, K. Thananjeyan, S. T. Yoganandham, *Inorg. Chem. Comm.*, **117**, 107954(1–7) (2020).

24. V. Tomar, T. F. Roberts, N. L. Abbott, J. P. Hernández-Ortiz, J. J. de Pablo, *Langmuir*, **28**, 6124–6131 (2012).
25. R. P. Pan, T. R. Tsai, C. Y. Chen, C. H. Wang, C. L. Pan, *Mol. Cryst. Liq. Cryst*., **409**, 137–144 (2004).
26. K. Tripathi, K. Mishra, S. M. Swadesh, K. Guptha, R. Manohar, *J. Mol. Struct*., **1035**, 371–377 (2013).
27. A. A. Ward, *State of the Art – Dielectric Materials for Advanced Applications*, National Research Centre, Egypt (2015).
28. M. M. Abdel-Aal, M. A. Ahmed, L. Ateya, *J. Phys. Soc. Jpn.*, **65**, 3351–3356 (1996).
29. A. K. Jonscher, *J. Phys. D: Appl. Phys*., **32**, 57–70 (1999).
30. C. C. Homes, S. M. Shapiro, T. Vogt, *Sciences*, **293**, 673–676 (2001).
31. A. J. Martin, G. Meier, A. Saupe, *Symp. Faraday Soc.,* **5**, 119–133 (1971).
32. G. Meir, A. Saupe, *Mol. Cryst. Liq. Cryst*., **1**, 515–525 (1996).
33. B. Bahadur, R. K. Sarna, V. G. Bhide, *Mol. Cryst. Liq. Cryst*., **88**, 151–165 (1982).